Augmentation of IFN-γ+ CD8+ T cell responses correlates with survival of HCC patients on sorafenib therapy

Suresh Gopi Kalathil,[1] Alan Hutson,[2] Joseph Barbi,[1] Renuka Iyer,[3] and Yasmin Thanavala[1]

[1]Department of Immunology, [2]Department of Biostatistics and Bioinformatics, and [3]Department of Medicine, Roswell Park Comprehensive Cancer Center, Buffalo, New York, USA.

BACKGROUND. Sorafenib has been shown to reduce the extent of immunosuppression in patients with hepatocellular carcinoma (HCC). The rationale of this investigation was to identify biomarkers that can predict treatment efficacy of sorafenib in HCC patients and to unravel the mechanism by which sorafenib impedes immune suppression mediated by distinct immunosuppressive cell subsets.

METHODS. With informed consent, blood samples were collected from 30 patients with advanced HCC, at baseline and 2 time points after initiation of sorafenib treatment. The frequency of PD-1+ T cells, ERK2 phosphorylation on flt-3+ Tregs and MDSCs, and T effector cell function were quantified by using flow cytometry.

RESULTS. Elevated levels of CD8+Ki67+ T cells producing IFN-γ were associated with improved progression-free survival and overall survival (OS). High frequencies of these T cells were correlated with significantly reduced risk of death over time. Patients with an increased pretreatment T effector/Treg ratio showed significant improvement in OS. ERK+flt-3+ Tregs and MDSCs were significantly decreased after sorafenib therapy. Increased numbers of baseline flt-3+p-ERK+ MDSCs were associated with survival benefit of patients.

CONCLUSION. A high baseline CD4+ T effector/Treg ratio is a potential biomarker of prognostic significance in HCC. CD8+Ki67+ T cells producing IFN-γ are a key biomarker of response to sorafenib therapy resulting in survival benefit. The immune modulation resulted from sorafenib-mediated blockade of signaling through the VEGF/VEGFR/flt-3 pathway, affecting ERK phosphorylation. These insights may help identify patients who likely would benefit from VEGFR antagonism and inform efforts to improve the efficacy of sorafenib in combination with immunotherapy.

TRIAL REGISTRATION. NCT02072486.

FUNDING. National Comprehensive Cancer Network Oncology Research Program from general research support provided by Bayer US LLC (NCCNSORA0002), National Cancer Institute grant P30CA016056, and pilot funds from Roswell Park Alliance Foundation.

Introduction

Hepatocellular carcinoma (HCC) is the most common primary liver cancer and the second leading cause of cancer-related death worldwide (1, 2). HCC arises from liver cirrhosis, with chronic infection by hepatitis B or C viruses as the leading cause, followed by other etiologies of cirrhosis, such as alcohol consumption and fatty liver disease associated with metabolic defect. Treatment options for advanced HCC are limited, rendering it a serious therapeutic challenge (3). Angiogenesis is one of the prerequisites of HCC progression, recurrence, and metastasis. Proangiogenic signaling through RAF/MEK/ERK cascade is critically important in angiogenesis and subsequent progression of HCC. Phosphorylated ERK (p-ERK), the key downstream component of this signal transduction pathway, is targeted by the oral multikinase inhibitor sorafenib, which is the mainstay of treatment for patients with HCC. Regorafenib, ramucirumab, cabozantinib, and lenvatinib are newly approved targeted antiangiogenic agents for the treatment of advanced HCC (4). Although sorafenib treatment results in improved

Conflict of interest: RI received consulting fees from Bayer.

Submitted: May 7, 2019
Accepted: June 27, 2019
Published: August 8, 2019.

Reference information: *JCI Insight*. 2019;4(15):e130116. https://doi.org/10.1172/jci.insight.130116.

progression-free survival (PFS) and overall survival (OS), treatment-associated toxicities are frequent, requiring dose interruptions and dose reductions for the majority of the patients. Conventional clinicopathological diagnostic tools used are inadequate to identify patients who will benefit from therapy. Therefore, there is an urgent need to develop novel biomarkers for predicting the prognosis of HCC patients undergoing sorafenib therapy.

Although the current immunotherapeutic approaches in patients with HCC have resulted in a favorable outcome, the relatively low response rates emphasize the strong immunosuppressive barriers that need to be circumvented by complementary immune-stimulatory approaches (5, 6). We and others have reported multiple redundant immunosuppressive mechanisms acting in concert to cause subversion of antitumor immunity in patients with advanced HCC (7, 8). Further, multipronged targeted depletion of suppressor cells resulted in the restoration of granzyme B production and proliferation of T cells (9, 10). Recently, we have also demonstrated that sorafenib treatment in patients with HCC beneficially reduces the extent of immune suppression caused by Tregs and programmed cell death-1–positive (PD-1$^+$) T cells, which correlated with OS (11). However, the effect of sorafenib treatment on cytotoxic T cell function from the perspective of HCC patient survival has not been elucidated. The role of VEGF in increasing immune checkpoint receptor PD-1 on tumor-specific T cells and downregulation of these receptors by blockade of the VEGF/VEGFR pathway has been clearly demonstrated in a mouse tumor model of colon cancer (12). Importantly, we have shown that blockade of the VEGF/VEGR2 pathway by using anti-VEGF antibody or in vitro exposure to sorafenib could decrease the frequency of PD-1$^+$ T cells in patients with HCC (11). The rationale of our current investigation was to elucidate the molecular mechanism by which sorafenib impedes immune suppression mediated by distinct immune cell subsets in the suppressive network. ERK is a key molecule in the signaling cascade of Tregs and myeloid-derived suppressor cell (MDSC) activation, and signaling via Fms-related tyrosine kinase 3 (flt-3) has been shown to be vital for the proliferation and expansion of human Tregs (13). Recently, it has been reported that sorafenib inhibits ERK activation and proliferation of flt-3–mutant acute myeloid leukemia cells (14, 15). We reasoned that ERK phosphorylation on flt-3$^+$ Tregs and MDSCs could be central to understanding the immunomodulatory action of sorafenib, and we therefore measured the levels of ERK phosphorylation on flt-3$^+$ Tregs and MDSCs of patients at the initiation of sorafenib treatment and multiple time points after treatment.

Furthermore, we hypothesized that if sorafenib impedes immunosuppressive mechanisms, it could enhance antitumor cytotoxicity of the patient's own effector T cells. Therefore, in this study, we examined whether reduction in the levels of immunosuppressive cell subsets following sorafenib treatment translates to a concomitant increase in T effector cell function and whether this is a functional biomarker of clinical benefit. The modulation of the immunosuppressive cell subsets and T cell function was measured serially during sorafenib therapy to determine whether improvement in immune function was sustained, which was the secondary scientific objective. Our study is the first to our knowledge to demonstrate the augmented cytotoxic potential of effector T cells following sorafenib treatment in patients with HCC. The field is rapidly evolving, with a number of antiangiogenic and immune checkpoint inhibitors being evaluated, making this work more relevant, with the potential to be translated to clinical practice and aid patient selection with a potentially novel and noninvasive immune biomarker of sorafenib efficacy.

Our studies suggest that treatment with sorafenib may delay tumor growth and metastases in patients with HCC not only by inhibiting angiogenesis but also by suppressing immunosuppressive cell subsets with concomitant activation of functional cytolytic T lymphocytes (CTL) producing IFN-γ and granzyme B. Our findings implicate sorafenib-mediated blockade of the VEGF/VEGFR/flt-3 signaling pathway, including ERK activation in immune suppressor cells, as a key molecular event in the immune modulation observed in patients with HCC benefiting from this therapy.

Results

Patient characteristics. We enrolled 39 patients for the study between November 2013 and May 2017 at Roswell Park Comprehensive Cancer Center, and 30 patients were evaluable for all biomarker endpoints (Figure 1). Clinical characteristics of patients are summarized in Table 1.

Clinical outcomes. Median 6-month PFS (primary endpoint for biomarkers) for Child-Pugh Class A and B was 0.42 (0.22–0.60) and 0.29 (0.09–0.52); median OS for Child-Pugh A and B was 9.2 (2.5–21.6)

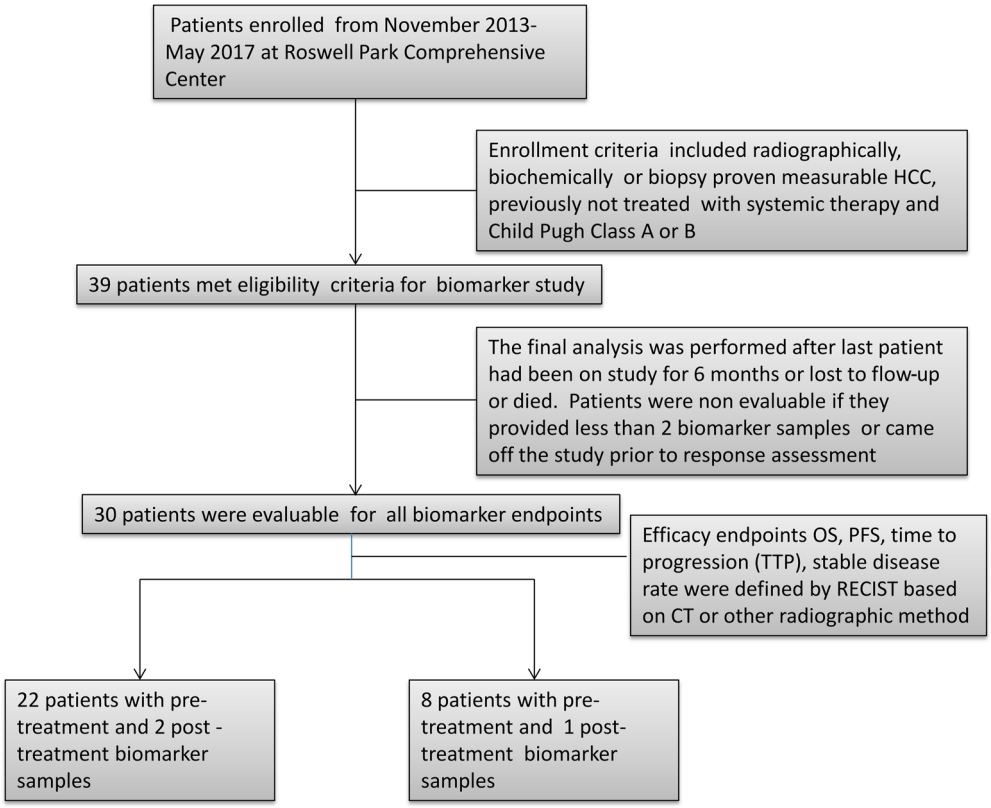

Figure 1. Description of cohorts for biomarker study. We recruited 39 patients for the study. Radiographically, biochemically, or biopsy-proven, measurable HCC that was not previously treated with systemic therapy and was Child-Pugh Class A or B were the eligibility criteria. The observation period for each patient was the time from the start of therapy with sorafenib to withdrawal of consent, death, or the last visit. Of the 39, 30 patients met eligibility criteria. One pretreatment and 2 posttreatment blood samples were collected for the biomarker study. Patients were nonevaluable for the primary biomarker endpoint if they provided fewer than 2 biomarker samples or came off the study before response assessment. Of 30 eligible patients, 22 provided 3 blood samples for biomarker study and 8 provided 2 blood samples. Response, dosing, and toxicity information were collected in a database, and deidentified biomarker data were analyzed in a blind fashion. PFS, progression-free survival.

months and 4.6 (1.3–11.3) months, respectively. No clinical predictors were significant at P value less than 0.05 in this small data set in predicting outcomes. These clinical outcomes in all 30 patients with paired biomarker samples were used for correlation with immune biomarkers as shown below. Study status and survival in relation to Child-Pugh score are summarized in Supplemental Tables 1 and 2, respectively; supplemental material available online with this article; https://doi.org/10.1172/jci.insight.130116DS1). No meaningful changes were seen in viral titers of patients with elevated titers at baseline, consistent with what others have reported, and no patients were on antivirals during sorafenib treatment (16).

Reduction in the frequency and number of Tregs and MDSCs following sorafenib treatment is associated with down-regulation of ERK phosphorylation. The levels of circulating $CD4^+Foxp3^+$ T cells and $CD14^-HLADR^-CD11b^+CD33^+$ MDSCs in patients with HCC were measured by flow cytometry before sorafenib therapy as well as at early (28–35 days) and late treatment (160 days) stages (Figure 2, A and D). Statistically significant reduction in the frequency (7.3% vs. 5.5%, $P = 0.001$, Figure 2B) and absolute number (9537 vs. 7603, $P = 0.05$, Figure 2C) of $CD4^+Foxp3^+$ Tregs and in the frequency (6% vs. 4.3% $P = 0.001$, Figure 2E) and absolute number (5836 vs. 4350, $P = 0.01$, Figure 2F) of $CD14^-HLADR^-CD11b^+CD33^+$ MDSCs was observed in blood samples collected at 28–35 days of sorafenib treatment as compared with pretreatment levels. Decreases in Tregs (7.3% vs. 5.7% $P = 0.01$, Figure 2B; 9537 vs. 6591, $P = 0.05$, Figure 2C) and MDSCs (6% vs. 3.8%, $P = 0.001$, Figure 2E; 5836 vs. 3727, $P = 0.01$, Figure 2F) were sustained up to after 160 days of treatment and were also statistically significant compared with baseline values. Further decreases in frequencies and absolute numbers did not occur beyond that measured at 28–35 days of treatment, except for the absolute number of MDSCs, which further decreased significantly (Figure 2, B, C, E, and F).

Table 1. Baseline characteristics of patients treated with sorafenib (n = 30)

Median age, years	**65 (56–84)**
Sex	
Male	26 (87%)
Female	4 (13%)
Race	
White	25 (83%)
African American	4 (13%)
Hispanic	1 (3%)
Median weight (kg)	79 (51–171)
Median height (cm)	174 (152–187)
Median BSA	1.9 (1.5–3.0)
Cause of disease	
Alcohol	11 (37%)
Hepatitis C virus	16 (53%)
Hepatitis B virus	2 (7%)
Nonalcoholic steatohepatitis	2 (7%)
Other	6 (20%)
ECOG performance status	
0	8 (27%)
1	21 (70%)
2	1 (3%)
Barcelona-Clinic Liver Cancer stage	
B	8 (27%)
C	22 (73%)
Child-Pugh liver function class	
A	20 (67%)
B	10 (33%)
Macrovascular invasion	18 (60%)

In addition to the decline in Treg frequencies and absolute numbers, importantly, there was a significant increase in the ratios of both $CD4^+CD127^+$ (5.1 vs. 7.4, P = 0.001, Figure 2G) and $CD8^+CD127^+$ (6.1 vs. 8.6, P = 0.001, Figure 2H) effector T cells (Teffs) to Tregs after sorafenib treatment. Enhancement in the ratios of $CD4^+$ Teffs and $CD8^+$ Teffs to Tregs was sustained for a long period after sorafenib treatment (5.1 vs. 7.9, P = 0.01, Figure 2G; 6.1 vs. 8.6, P = 0.05, Figure 2H). Mitigation of Tregs and MDSCs and subsequent enhancement in the Teff/Treg ratio following sorafenib therapy that were long-lasting likely contribute to antitumor immune responses in these patients.

Coupled with diminution of Tregs and the MDSC population, a significant reduction in the levels of ERK phosphorylation was observed on $flt\text{-}3^+$ Tregs and MDSCs after sorafenib treatment. We found that the frequency (65.5% vs. 50.5%, P = 0.001, Figure 2, I and J) and absolute number (383.5 vs. 233, P = 0.06, Figure 2K) of $flt\text{-}3^+$ $p\text{-}ERK^+$ Tregs and frequency (87.1% vs. 73.9%, P = 0.001, Figure 2, L and M) and absolute number (396 vs. 244.7, P = 0.01, Figure 2N) of $flt\text{-}3^+p\text{-}ERK^+$ MDSCs were significantly decreased in samples collected 28–35 days after initiation of sorafenib treatment. Decreased ERK phosphorylation levels on Tregs (65.5% vs. 37.62%, P = 0.001, Figure 2J; 383.5 vs. 169.4, P = 0.01, Figure 2K) and MDSCs (87.1% vs. 70.5%, P = 0.001, Figure 2M; 396 vs. 176, P = 0.01, Figure 2N) were also monitored at the second follow-up measurement after 160 days of sorafenib treatment. p-ERK is a key downstream target of sorafenib and could therefore serve as a potential biomarker of its efficacy. Our studies show that signaling via flt-3 receptor on Tregs and MDSCs is inhibited by sorafenib, resulting in the downregulation of ERK phosphorylation, implicating this as a potential mechanism by which sorafenib inhibits suppressive Tregs and MDSCs in patients with HCC. Eight of thirty patients had died before the second posttreatment blood draw (160 days), and immune profiles of these patients at 28–35 days combined with surviving patients (n = 22 + 8) have been summarized in Supplemental Figure 1. A comparison of the peripheral blood immune cell population with intrahepatic immune cell subsets could not be performed in this small cohort of 30 patients with advanced disease who presented with poor liver function because tumor biopsies for translational studies could have affected their current standard of care or quality of life. We acknowledge this as a limitation of our study.

Reduction in $Foxp3^+$ Tregs coexpressing CTLA-4 and neuritin after sorafenib treatment. Our characterization of the pre- and posttreatment HCC patient samples demonstrated that the frequency of $Foxp3^+CTLA\text{-}4^+$ Tregs was significantly reduced after sorafenib therapy (4.3% vs. 3.5%, P = 0.01, Figure 3, A and B). However, absolute number of $Foxp3^+CTLA\text{-}4^+$ Tregs did not show any significant decrease (Figure 3C). In addition to reducing the frequency of Tregs expressing CTLA-4, in a subset of patients, sorafenib treatment also decreased the frequency of Tregs coexpressing the neurotrophic factor known as neuritin on their surface (40.5% vs. 24.5%, P = 0.01, Supplemental Figure 2, A and B), a molecule implicated as a Treg-associated factor and relevant to an activated Treg phenotype. The frequency of $neuritin^+$ Tregs in HCC patients' pretreatment samples was also significantly higher than age-matched healthy subjects (40.5% vs. 14.3%, P = 0.001, Supplemental Figure 2B). Thus, neuritin may be an additional marker of Tregs responsible for dampening antitumor immunity in HCC patients who are also susceptible to therapeutic disruption of VEGF/VEGFR signaling.

Reduction in T cell exhaustion following treatment with sorafenib. We further examined the expression levels of immune checkpoint receptor PD-1, a molecular signature of T cell exhaustion on activated T cells,

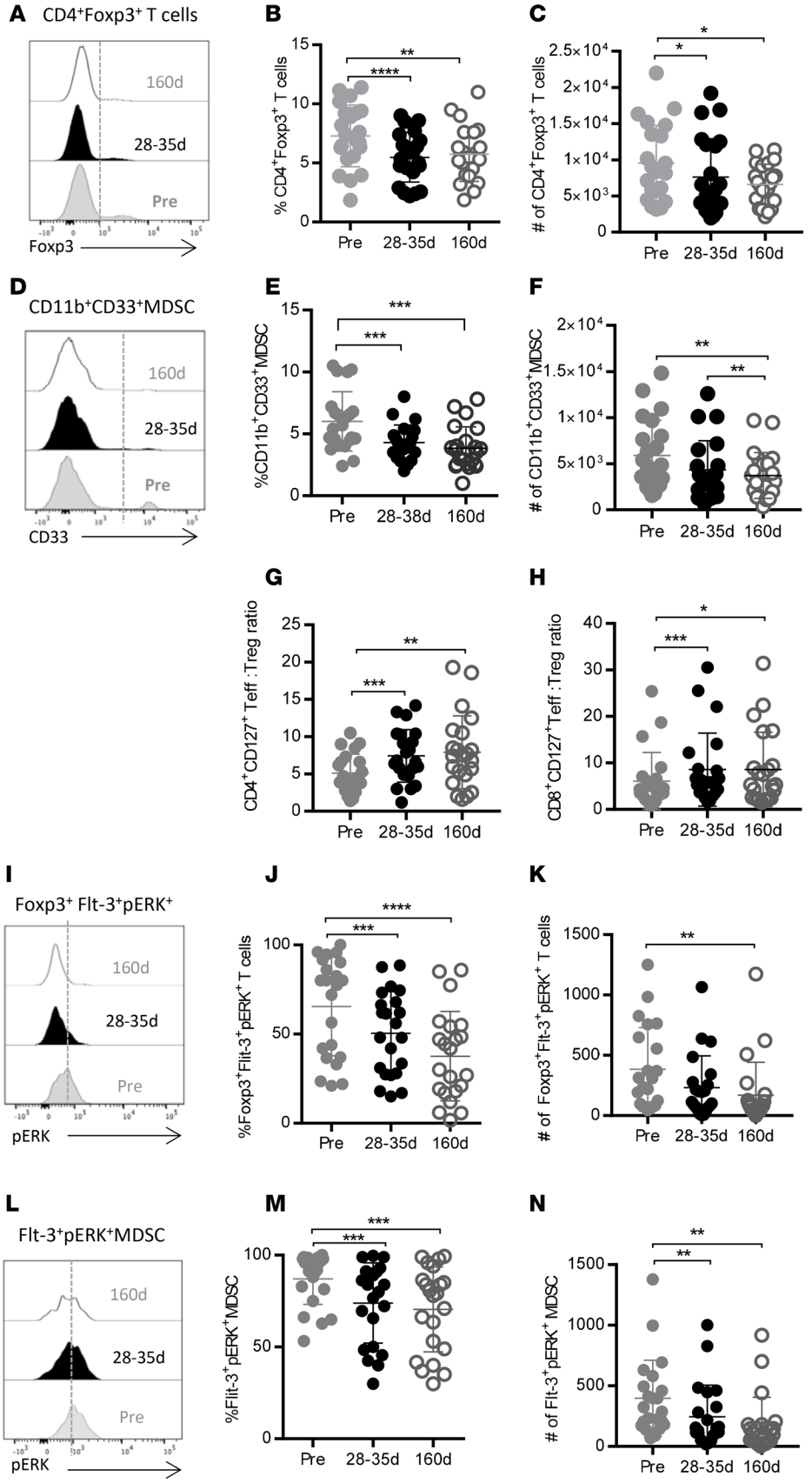

Figure 2. Reduction in immunosuppressive cell subsets after sorafenib therapy. Frequencies of various immune T cell subsets were calculated on live $CD3^+CD4^+$ or $CD3^+CD8^+$ T cell populations and MDSCs are $CD14^-HLA\text{-}DR^-CD11b^+CD33^+$. Absolute number is cells per milliliter. (**A**) Representative histogram offset showing the frequency of $CD4^+Foxp3^+$ Tregs measured at pretreatment and after 28–35 days and 160 days of sorafenib treatment. (**B**) Frequency and (**C**) absolute numbers of $CD4^+Foxp3^+$ Tregs pretreatment and after 28–35 days and 160 days (n = 22). (**D**) Representative histogram offset showing frequency of $CD11b^+CD33^+$ MDSCs measured at pretreatment and after 28–35 days and 160 days of sorafenib treatment. (**E**) Frequency and (**F**) absolute numbers of MDSCs pretreatment and after 28–35 days and 160 days (n = 22). (**G**) Ratio of $CD4^+CD127^+$ T cells to $CD4^+Foxp3^+$ T cells ($CD4^+CD127^+$ T cells/$CD4^+Foxp3^+$ T cells) pretreatment and after 28–35 days and 160 days (n = 22). (**H**) Ratio of $CD8^+CD127^+$ T cells to $CD4^+Foxp3^+$ T cells pretreatment and after 28–35 days and 160 days (n = 22). (**I**) Representative histogram offset, showing frequency of $Foxp3^+flt\text{-}3^+p\text{-}ERK^+$ Tregs measured at pretreatment and after 28–35 days and 160 days of sorafenib treatment. (**J**) Frequency and (**K**) absolute numbers of $Foxp3^+flt\text{-}3^+p\text{-}ERK^+$ Tregs measured at pretreatment and after 28–35 days and 160 days of sorafenib treatment (n = 22). (**L**) Representative histogram offset, showing frequency of $flt\text{-}3^+p\text{-}ERK^+$ MDSCs measured at pretreatment and after 28–35 days and 160 days of sorafenib treatment. (**M**) Frequency and (**N**) absolute numbers of $flt\text{-}3^+p\text{-}ERK^+$ MDSCs pretreatment, 28–35 days, and 160 days (n = 22). Each symbol represents an individual HCC patient. Error bars represent mean ± standard deviation (SD). $^{****}P < 0.0001$; $^{***}P < 0.001$; $^{**}P < 0.01$; $^{*}P < 0.05$; paired t test.

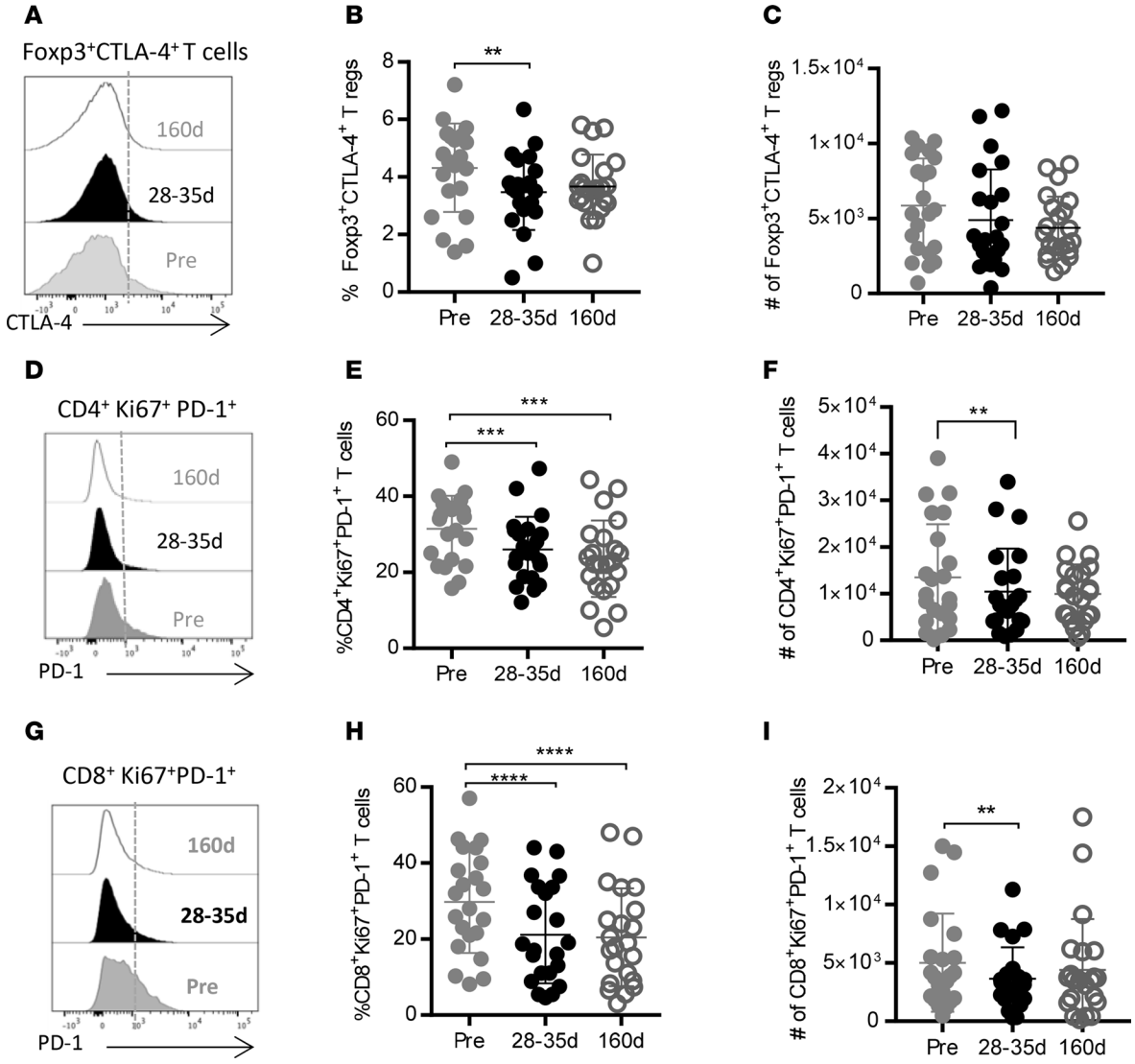

Figure 3. Decrease in T cell exhaustion markers after sorafenib treatment. Immunophenotypic analysis of T cells was performed after stimulation of PBMCs in vitro using anti–CD3/CD28 at pretreatment and after 28–35 days and 160 days of sorafenib treatment by multicolor flow cytometry. Frequencies of various immune cell subsets were calculated on live $CD3^+CD4^+$ or $CD3^+CD8^+$ T cell populations, and absolute number is cells per milliliter. (**A**) Representative histogram offset showing frequency of $Foxp3^+CTLA\text{-}4^+$ Tregs measured at pretreatment and after 28–35 days and 160 days of sorafenib treatment. (**B**) Frequency and (**C**) absolute numbers of $Foxp3^+CTLA\text{-}4^+$ Tregs pretreatment, 28–35 days, and 160 days (n = 22). (**D**) Representative histogram offset showing frequency of $CD4^+Ki67^+PD\text{-}1^+$ T cells measured at pretreatment and after 28–35 days and 160 days of sorafenib treatment. (**E**) Frequency and (**F**) absolute number of $CD4^+Ki67^+PD\text{-}1^+$ T cells pretreatment, 28–35 days, and 160 days (n = 22). (**G**) Representative histogram offset showing frequency of $CD8^+Ki67^+PD\text{-}1^+$ T cells measured at pretreatment and after 28–35 days and 160 days of sorafenib treatment. (**H**) Frequency and (**I**) absolute number of $CD8^+Ki67^+PD\text{-}1^+$ T cells pretreatment, 28–35 days, and 160 days (n = 22). Each symbol represents an individual HCC patient. Error bars represent mean ± standard deviation (SD). $^{****}P < 0.0001$; $^{***}P < 0.001$; $^{**}P < 0.01$; paired t test.

during sorafenib treatment in patients with HCC. A significant reduction in the frequency (31.5% vs. 26%, $P = 0.001$, Figure 3, D and E) as well as absolute number (13,508 vs. 10,460, $P = 0.01$, Figure 3F) of $CD4^+Ki67^+PD\text{-}1^+$ T cells and in the frequency (29.8% vs. 21%, $P = 0.001$, Figure 3, G and H) and absolute number (5025 vs. 3643, $P = 0.01$, Figure 3I) of $CD8^+Ki67^+PD\text{-}1^+$ T cells was observed 28–35 days after sorafenib treatment as compared with pretreatment levels. Of note, the frequency of $CD4^+PD1^+$ T cells (31.5% vs. 23.6%, $P = 0.001$, Figure 3E) and $CD8^+PD1^+$ T cells (29.8% vs. 20.5%, $P = 0.001$, Figure 3H) remained significantly low in the follow-up blood samples collected after 160 days of treatment, demonstrating that sorafenib-mediated downregulation of this inhibitory checkpoint on T cells was sustained for a prolonged period. Profiles of immune checkpoint receptors at 28–35 days of 8 patients who had died before the second posttreatment blood draw (160 days) combined with surviving patients (n = 22 + 8) have

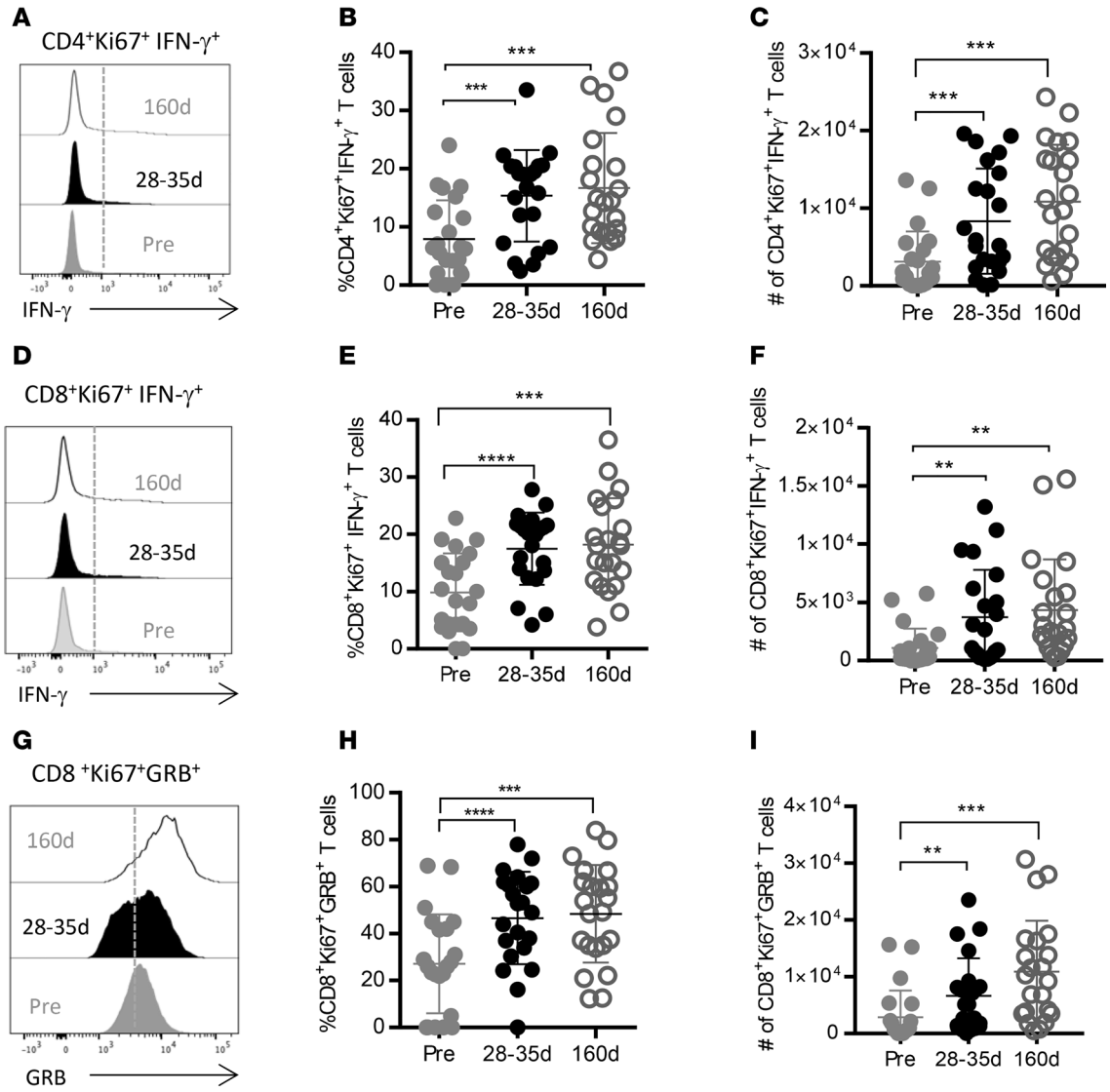

Figure 4. Effect of sorafenib treatment on Teffs. PBMCs from patients with HCC were stimulated with anti–CD3/CD28 in vitro for 48 hours and immunophenotypic analysis was performed. Frequencies of various immune cell subsets were calculated on live $CD3^+CD4^+$ or $CD3^+CD8^+$ T cell populations, and absolute number is cells per milliliter. (**A**) Representative histogram offset showing frequency of $CD4^+Ki67^+IFN\text{-}\gamma^+$ T cells measured at different time points of sorafenib treatment. (**B**) Frequencies and (**C**) absolute number of $CD4^+Ki67^+IFN\text{-}\gamma^+$ T cells pretreatment, 28–35 days, and 160 days (n = 22). (**D**) Representative histogram offset showing frequency of $CD8^+IFN\text{-}\gamma^+$ T cells measured at different time points of sorafenib treatment. (**E**) Frequencies and (**F**) absolute number of $CD8^+Ki67^+IFN\text{-}\gamma^+$ T cells pretreatment, 28–35 days, and 160 days (n = 22). (**G**) Representative histogram offset showing frequency of $CD8^+Ki67^+GRB^+$ T cells measured at different time points of sorafenib treatment. (**H**) Frequencies and (**I**) absolute number of $CD8^+Ki67^+GRB^+$ T cells pretreatment, 28–35 days, and 160 days (n = 22). Each symbol represents an individual HCC patient. Error bars represent mean ± standard deviation (SD). $^{****}P < 0.0001$; $^{***}P < 0.001$; $^{**}P < 0.01$; paired t test.

been summarized in Supplemental Figure 3. Our results underscore that immune checkpoint inhibitor therapy combined with sorafenib could generate a synergistic effect and may favor better clinical outcome in patients with HCC.

In addition to $Foxp3^+$ Tregs, expression of neuritin has also been linked to anergic $CD8^+$ and $CD4^+$ T cell populations. We found that in patients with HCC, the frequency of $CD4^+PD\text{-}1^+$ T cells coexpressing neuritin was significantly higher than in normal healthy subjects, suggesting a role for these cells in liver cancer–associated immune dysfunction (33% vs. 21.3%, $P = 0.05$, Supplemental Figure 2, C and D). Notably, these cells were significantly reduced after sorafenib treatment (33% vs. 19.6%, $P = 0.05$, Supplemental Figure 2D). Neuritin expression on $CD8^+PD\text{-}1^+$ T cells was similarly reduced after sorafenib therapy (35.3% vs. 17.8%, $P = 0.01$, Supplemental Figure 2, E and F). This decline in $PD\text{-}1^+$neuritin$^+$ T cells, potentially exhausted or anergic populations capable of attenuating antitumor

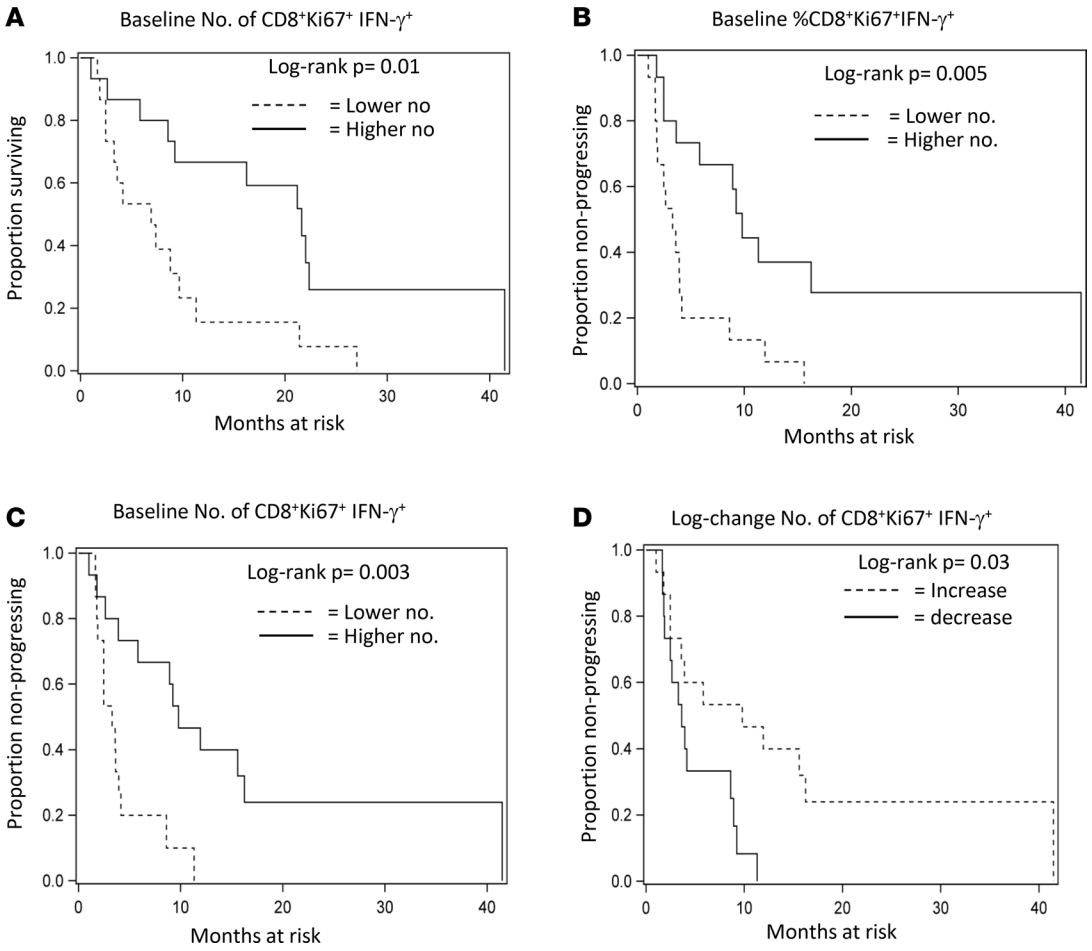

Figure 5. Kaplan-Meier plots showing both the predictive immune correlates of response to and efficacy of sorafenib treatment in patients with HCC. Plots **A**–**C** show the correlation between $CD8^+Ki67^+IFN\text{-}\gamma^+$ T cells before sorafenib treatment (baseline values) and patient survival. The association between $CD8^+Ki67^+IFN\text{-}\gamma^+$ T cells and OS or PFS was calculated as described in Methods. (**A**) Absolute numbers of baseline values of $CD8^+Ki67^+IFN\text{-}\gamma^+$ T cells and OS. (**B**) Frequency of $CD8^+Ki67^+IFN\text{-}\gamma^+$ T cells at baseline and PFS. (**C**) Absolute numbers of $CD8^+Ki67^+IFN\text{-}\gamma^+$ T cells and PFS. (**D**) Log change in absolute numbers of $CD8^+Ki67^+IFN\text{-}\gamma^+$ T cells (log of the ratio [post/pre] and PFS).

immune responses in HCC, may be partly attributed to a hitherto-unanticipated susceptibility of these populations to VEGFR signaling antagonism.

Enhanced IFN-γ production and proliferation of effector $CD4^+$ and $CD8^+$ T cells in patients treated with sorafenib. Teff proliferation and IFN-γ production were evaluated at 3 time points during sorafenib treatment: before treatment initiation and at 28–35 days and 160 days after commencement of treatment. Stimulation of PBMCs in vitro using anti–CD3/CD28 resulted in the generation of significantly increased frequency (7.9% vs. 15.3%, $P = 0.001$, Figure 4, A and B) as well as absolute number of $CD4^+Ki67^+IFN\text{-}\gamma^+$ T cells (3101 vs. 8314, $P = 0.001$, Figure 4C) and significantly high frequency (9.9% vs. 17.5%, $P = 0.001$, Figure 4, D and E) and absolute number of $CD8^+Ki67^+IFN\text{-}\gamma^+$ T cells (1094 vs. 3731, $P = 0.001$, Figure 4F) after 28–35 days of sorafenib treatment as compared with the pretreatment sample. We observed significantly higher frequencies as well as absolute numbers of proliferating $CD4^+Ki67^+$ (7.9% vs. 16.7%, $P = 0.001$, Figure 4B; 3101 vs. 10,865, $P = 0.001$, Figure 4C) and $CD8^+Ki67^+$ T cells (9.9% vs. 18.2%, $P = 0.001$, Figure 4E; 1094 vs. 4353, $P = 0.001$, Figure 4F) producing IFN-γ even at a later stage of treatment in surviving patients, highlighting the durability of the sorafenib-induced immune modulatory effect in HCC. Profiles of T cell IFN-γ production by 8 patients who had passed away before the second posttreatment blood draw combined with surviving patients ($n = 22 + 8$) have been summarized in Supplemental Figure 4.

Increased expression of granzyme B by proliferating cytotoxic T cells in patients treated with sorafenib. Further, we investigated the expression of granzyme B, a mediator of target cell lysis by CTLs in cell-mediated immune responses, at different time intervals during the course of treatment. Activated $CD8^+$ T cells showed a sig-

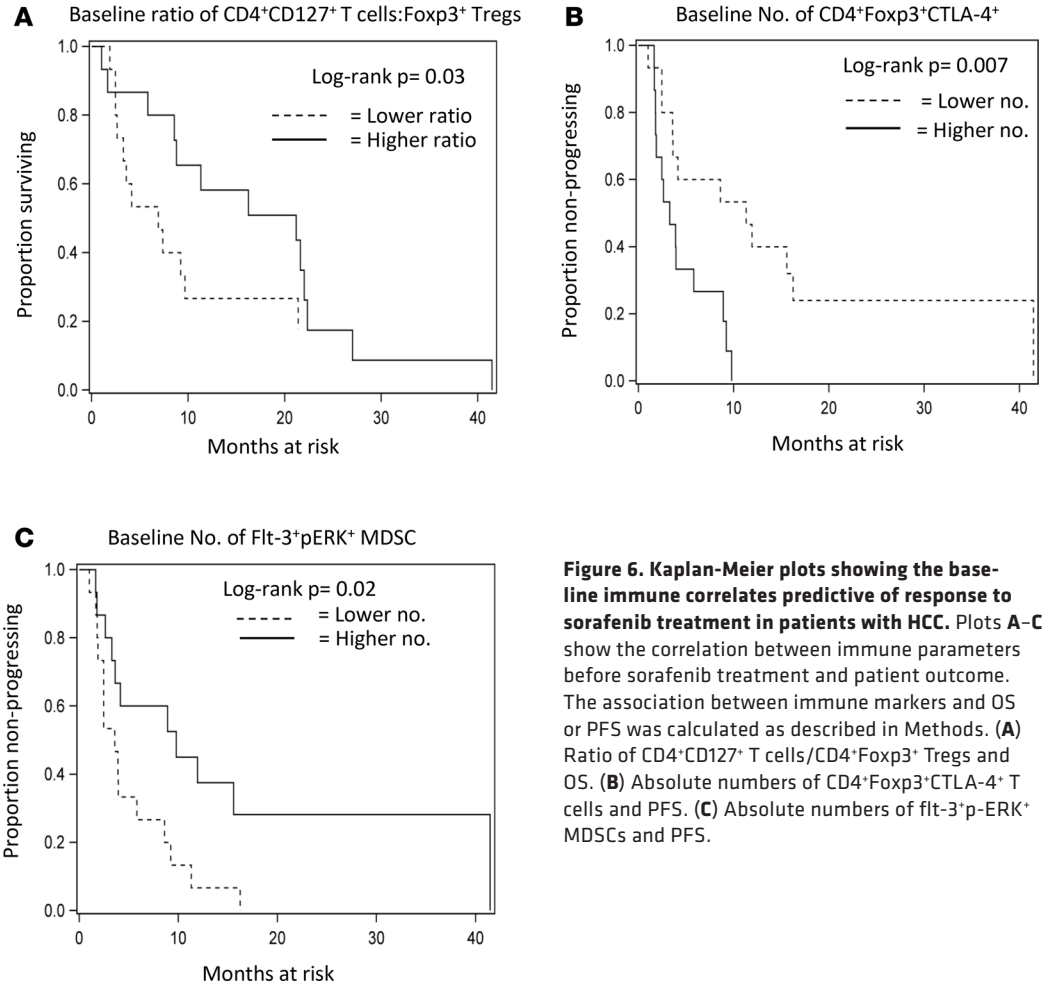

Figure 6. Kaplan-Meier plots showing the baseline immune correlates predictive of response to sorafenib treatment in patients with HCC. Plots **A**–**C** show the correlation between immune parameters before sorafenib treatment and patient outcome. The association between immune markers and OS or PFS was calculated as described in Methods. (**A**) Ratio of $CD4^+CD127^+$ T cells/$CD4^+Foxp3^+$ Tregs and OS. (**B**) Absolute numbers of $CD4^+Foxp3^+CTLA\text{-}4^+$ T cells and PFS. (**C**) Absolute numbers of flt-3^+p-ERK^+ MDSCs and PFS.

nificant increase in the frequency as well as absolute numbers of $Ki67^+$granzyme B^+ CTLs in blood samples collected 28–35 days (27.2% vs. 46.6%, $P = 0.001$, Figure 4, G and H; 2870 vs. 6631, $P = 0.01$, Figure 4I) and 160 days (27.2% vs. 48.4%, $P = 0.001$, Figure 4H; 2870 vs. 10,910, $P = 0.001$, Figure 4I) after initiation of sorafenib treatment as compared with pretreatment samples. Profiles of granzyme B^+CD8^+ T cells at 28–35 days from 8 patients who had died before the second posttreatment blood draw combined with surviving patients ($n = 22 + 8$) are summarized in Supplemental Figure 4.

Predictive and prognostic immune correlates of survival in patients with HCC. OS of patients was significantly affected by the absolute numbers of IFN-γ–producing $CD8^+Ki67^+$ T cells before treatment initiation (log-rank $P = 0.01$, Figure 5A). Both the frequencies and absolute numbers of this phenotype showed significant association with PFS (log-rank $P = 0.005$, Figure 5B; log-rank $P = 0.003$, Figure 5C). Furthermore, patients with an increase in the absolute numbers of this phenotype quantified after sorafenib therapy had improved PFS (log-rank $P = 0.03$, Figure 5D). Importantly, high frequencies of $CD8^+Ki67^+IFN\text{-}\gamma^+$ T cells were also associated with significantly reduced risk of death over time (hazard ratio = 0.33; $P = 0.005$). Collectively, our results highlight that $CD8^+Ki67^+$ T cells producing IFN-γ may represent a key immune subset defining response to sorafenib treatment.

Patients with high pretreatment Teff/Treg ratio achieved significant improvement in OS (log-rank $P = 0.03$, Figure 6A). In corroboration of this finding, we also show that patients with low numbers of baseline $Foxp3^+CTLA\text{-}4^+$ Tregs had improved PFS (log-rank $P = 0.007$, Figure 6B).

Pretreatment levels of the absolute number of flt-3^+p-ERK^+ MDSCs showed significant correlation with PFS of patients (log-rank $P = 0.02$, Figure 6C). In concordance with earlier studies reporting increased responsiveness of HCC patients with high baseline p-ERK^+ tumors to sorafenib treatment, our HCC patients with increased numbers of baseline p-ERK^+ MDSCs may be more susceptible to VEGFR signaling antagonism. Although there are multiple strategies that tumor cells use, MDSCs are a key driver

of tumor-mediated immune evasion, and targeting MDSCs in immunotherapy appears to be a promising strategy with clinical relevance for patients with HCC.

Discussion

Even though presently sorafenib remains the gold standard of treatment for advanced, unresectable HCC and provides modest improvement in survival, treatment options for HCC are increasing, and patient selection will soon be a clinical challenge. Based on preclinical and human studies, sorafenib in addition to having an antiangiogenic property has been shown to beneficially modulate the extent of the immunosuppressive network in patients with HCC (11). The rationale of the present study was to delineate the molecular events responsible for the beneficial immune modulation mediated by sorafenib and to interrogate whether reduction in immunosuppressive cell subsets translates into concomitant improvement in cell-mediated immune function measured as enhanced proliferation and IFN-γ and granzyme B production by CTLs. These biomarkers with strong predictive and prognostic value either at pretreatment or early treatment could have translational potential for selecting individualized treatment options for patients or providing justification for prolonged sorafenib treatment.

The decrease in the frequency and absolute number of redundant immunosuppressive phenotypes observed in patients after sorafenib therapy further supports our earlier report on patients with HCC treated with sorafenib (11). Immunomodulatory properties of sorafenib have been studied using mouse tumor models of HCC. Based on these studies, sorafenib has been shown to reduce PD-1$^+$CD8$^+$ T cell number and inhibit proliferation and suppressive properties of Tregs and MDSCs (17, 18). In patients with HCC treated with sorafenib, a significant reduction in the number of tumor-infiltrating Tregs in the liver tissue with concomitant downregulation of TGF-β has been reported; a subpharmacological dose of sorafenib in vitro has been shown to enhance Teff proliferation and IL-2 production with downmodulation of Treg function (19, 20). By using paired pre- and posttreatment samples at 2 time points from patients with HCC, we performed a comprehensive analysis of the dynamic levels of circulating immunosuppressive cell subsets. The serial monitoring of suppressive phenotypes, Tregs, MDSCs, and inhibitory checkpoints during treatment revealed that sorafenib's immune-modulating effects were sustained over 160 days when second follow-up measurements were made.

In the present study, a significant reduction in the levels of ERK phosphorylation was noted in flt-3$^+$ Tregs and MDSCs after sorafenib treatment. Patients with a higher number of baseline flt-3$^+$p-ERK$^+$ MDSCs achieved improvement in PFS; these patients appeared to be more responsive to sorafenib-mediated intervention in the VEGF/VEGFR signaling pathway. Susceptibility of flt-3$^+$p-ERK$^+$ MDSCs to sorafenib therapy supports the potential link between VEGF signaling and MDSCs, a suppressor cell subset well known for the subversion of antitumor immunity through induction of Tregs and inhibitory cytokines. Sorafenib is an inhibitor of several serine and threonine kinases, such as RAF, and tyrosine kinases, including VEGFRs. Sorafenib has been shown to block ERK activity and proliferation of flt-3–mutant acute myeloid leukemia cells (14, 15) and reduce ERK phosphorylation of endothelial progenitor cells from patients with HCC (21). Activated ERK is a key downstream component of this signaling cascade that sorafenib is targeting. In a phase II study using tumor biopsies from patients with HCC (22) and another recent study using an HCC patient–derived xenograft model, it has been shown that tumors with high baseline p-ERK levels are more responsive to sorafenib treatment (23).

The inherent tolerogenic nature of the liver likely impedes an effective antitumor immune response to eliminate hepatic tumor cells at an early stage of development. Additionally, immune surveillance in HCC is subverted by immunosuppressive cytokines IL-10 and TGF-β, which are upregulated with concomitant downregulation of proinflammatory IFN-γ levels (8). The immune checkpoint receptor PD-1 is a major contributor to the subversion of antitumor immunity in the hepatic microenvironment and has become a novel therapeutic target for HCC. Clinical trials validating the therapeutic potential of checkpoint inhibitors blocking the PD-1 axis either alone or in combination with sorafenib are underway in patients with HCC, and nivolumab showed a manageable safety profile with durable objective responses in a subset of patients and was approved by the FDA for second-line therapy following failure of sorafenib (6, 24, 25). Although the comparative, randomized phase III trial of nivolumab versus sorafenib as first-line therapy (CheckMate 459) is complete and will report soon, our finding that sorafenib treatment results in sustained reductions of PD-1$^+$ T cells in patients with HCC suggests that a combination of PD-1 blockade and sorafenib could have

a synergistic effect in patients with HCC and potentially may lead to a better outcome in those patients who develop sorafenib resistance after long-term exposure. This theory has been validated in a small 23-patient study combining atezolizumab and bevacizumab reported at ASCO 2018 (26). VEGF-induced upregulation of PD-1 expression on tumor-specific T cells and mitigation of PD-1 expression by intervention in the VEGF/VEGFR pathway have been demonstrated in a mouse model of colon cancer (12). Our studies in a different cohort of 22 patients with HCC have shown that a decrease in the expression levels of PD-1 on T cells after sorafenib treatment is associated with survival benefit, and blockade of the VEGF/VEGR2 pathway or exposure to sorafenib in vitro reduces PD-1 expression levels on T cells (11). These studies provide insight into the appropriate molecular-targeted agent that may be used in combination with immune checkpoint inhibitors for the treatment of HCC.

Consistent with our hypothesis, reduction of additive suppressive phenotypes after sorafenib treatment was associated with reinvigoration of antitumor immune responses in patients. In the current study, the reversal of T cell exhaustion was reflected by marked reduction in the expression levels of coinhibitory receptors PD-1 and CTLA-4 on T cells following 4 weeks of treatment that was sustained over a prolonged period. Decreased number of baseline Tregs coexpressing checkpoint receptor CTLA-4 showed significant correlation with improvement in PFS. Tregs coexpressing markers of activation or immune checkpoints have been reported to be associated with worse prognosis in many cancers (27). Recently, using a clinically relevant mouse xenograft model of HCC, it has been shown that treatment with tyrosine kinase inhibitor sunitinib resulted in the priming of antitumor immune response by significantly decreasing Treg frequency (28). An important aspect of our mechanistic study was that we also performed a comprehensive analysis on kinetics of T cell function by using paired samples from patients at 3 time points. In the current study, we also observed a significant sorafenib-mediated reduction in the frequency of circulating neuritin$^+$ Tregs, a subpopulation enriched in patients with HCC relative to healthy donors. The gene encoding this neurotrophin (Nrn1) has been reported by several groups to be among those upregulated in Tregs relative to conventional T cell populations (29–32) or on Tregs under the control of their canonical transcription factor, Foxp3 (32, 33). Moreover, neuritin expression was recently noted among a subset of Tregs with an activated phenotype (34, 35). Although the role of neuritin in Treg biology remains to be fully defined, its expression on Tregs that are enriched in patients with HCC supports the notion that this molecule may indeed be a marker for human Tregs participating in the suppression of effective antitumor immunity in this deadly cancer type. Additionally, the apparent susceptibility of neuritin-expressing Tregs to sorafenib therapy further suggests a link among this factor, VEGF signaling in Tregs, and a subset of suppressor cells now widely appreciated to be tumor abetting (i.e., activated Tregs) (34, 36, 37). Recently, neuritin expression was also reported among anergic CD8$^+$ and CD4$^+$ T cells (38, 39). In line with a role for this molecule in the dysfunctional T cell response to liver cancer, we found a prominent population of T cells coexpressing neuritin and the exhaustion/anergy marker PD-1. Notably, these cells were significantly reduced in patients with HCC by sorafenib therapy. Our findings call attention to the potential role of neuritin in Treg- and exhaustion-driven immune tolerance in HCC, and they encourage further exploration of the factor as a potentially novel therapeutic target in the silencing of Tregs in the cancer setting.

Studies based on gene expression profiles in a cohort of 956 patients with HCC have demonstrated that 25% of these patients express enrichment of signatures identifying CD8$^+$ T cells, IFN-signaling genes, and markers of cytolytic activity. Furthermore, this group of patients had improved OS (40). Sorafenib has been shown to enhance graft versus leukemia activity through activation of CD8$^+$CD107$^+$IFN-γ^+ T cells in patients with flt-3 ITD mutant acute myeloid leukemia cells (41). In the above paper, authors have shown that the activation of CD8$^+$CD107$^+$IFN-γ^+ T cells by sorafenib is mediated via reduced ATF4 expression, causing activation of the IRF7/IL-15 axis in leukemia cells leading to metabolic reprogramming of leukemia-reactive T cells. In the current study, concomitant with an inhibitory effect on multiple suppressive cell subsets, we demonstrate that sorafenib treatment in patients with HCC resulted in the functional restoration of Teffs, evidenced by enhancement in the Teff/Treg ratio and increased IFN-γ and granzyme B production by CD4$^+$ and CD8$^+$ T cells following T cell receptor ligation. A further aspect of T cell functionality, namely the proliferative capacity of T cells upon TCR ligation, was also enhanced following sorafenib treatment. Of clinical relevance, increased frequencies or absolute numbers of CD8$^+$Ki67$^+$IFN-γ^+ T cells were associated with significantly improved survival of the patients with HCC. Importantly, high frequencies of CD8$^+$Ki67$^+$ T cells producing IFN-γ were implicated in significantly lowering risk of death over time.

Consistent with our data, earlier studies have also shown the inhibitory effect of sorafenib on ERK

phosphorylation and proliferation of flt-3–mutant leukemia cells (14, 15). Tyrosine kinase inhibitors, such as dasatinib and imatinib, have been shown to impede immune escape mechanisms in patients with CML by downregulation of MDSCs, simultaneously increasing T cell IFN-γ production (42). In another study, dasatinib treatment increased the number of granzyme B–producing $CD4^+$ and $CD8^+$ memory T cells in patients with CML, which functionally differentiated into Th1-type T cells capable of producing IFN-γ (43). In our study, we observed high baseline Teff/Treg ratio significantly affected OS of patients. High Treg/Teff ratios in the tumor microenvironment have been reported to be associated with poor prognosis in different types of malignancies (27). In patients with gastrointestinal stromal tumor (GIST) treated with imatinib, greater intratumoral $CD8^+$ T cell/Treg ratio was correlated with sensitivity of tumors to imatinib and IDO expression. Thus $CD8^+$ T cells were thought to be critical to the antitumor effects of targeted therapy in GIST (44).

In conclusion, our studies reveal the central role of $CD8^+$ T cells in this targeted therapy for liver cancer, and they suggest that $CD8^+Ki67^+IFN\text{-}\gamma^+$ cells may be a viable immune biomarker for the treatment efficacy of sorafenib in patients with HCC. Furthermore, we show that a high baseline $CD4^+$ Teff/Treg ratio may be a biomarker of prognostic significance in HCC. Importantly, our results provide the scientific rationale for combining sorafenib with checkpoint inhibitors. Such a regimen should be capable of both targeting tumor angiogenesis and downregulating suppressor cell phenotypes, an "off-target" effect of sorafenib on the immune system. With several recent successful studies of targeted antiangiogenic agents (ramucirumab, cabozantinib, lenvatinib) and effective treatment for hepatitis C, the HCC landscape is rapidly changing (4). Biomarkers that help predict benefit and reduce exposure to toxic therapies would have a significant effect on cost, quality of life, and patient survival. These agents can potentially synergize to reignite antitumor immunity in patients with HCC and improve the magnitude and durability of antitumor responses, and appropriate biomarkers may aid selections of therapy sequence and be paradigm changing for this disease.

Methods

This study was based on a clinical trial (NCT02072486) conducted in patients with advanced HCC at the Roswell Park Comprehensive Cancer Center (RPCCC) enrolled between November 3, 2013, and November 24, 2017. The study included patients with (a) radiographically, biochemically, or biopsy-proven, measurable HCC (b) that was previously not treated with systemic therapy for advanced disease of (c) Child-Pugh Class A or B who were deemed candidates for sorafenib therapy. Starting dose and dose adjustments were made according to the package insert. The observation period for each patient was the time from the start of therapy with sorafenib to withdrawal of consent, death, or the last visit. Response, dosing, and toxicity information were collected in a database, and deidentified biomarker data were analyzed in blinded fashion and entered into the database for statistical analysis. No interim data analyses for safety monitoring were planned because treatment was the standard of care. The final analysis occurred after the last patient had been in the study for 6 months or was lost to follow-up or died. Patients were nonevaluable for the primary biomarker endpoint if they provided fewer than 2 biomarker samples or came off the study before response assessment. Efficacy endpoints of OS, time to progression, PFS, response rate, and stable disease rate were defined by RECIST based on CT or other equivalent radiographic method at baseline and at follow-up visits every 8 weeks. Common Terminology Criteria for Adverse Events grade, action taken, and outcome were recorded.

Patients. Over a 4-year period, 39 eligible patients were consented, 30 of which were evaluable for all biomarker endpoints, and all treated patients were included in the toxicity assessment.

Biomarker analysis. Heparinized peripheral blood samples were obtained from patients with HCC before the initiation of treatment and after 28–35 days and 160 days of sorafenib treatment. PBMCs were isolated by Ficoll-Paque density gradient centrifugation and cryopreserved (8). Functional studies on T cells were carried out after in vitro stimulation of PBMCs in the presence of 1 μg/mL anti-CD3 antibody (clone OKT3; BD Biosciences) and 0.5 μg/mL anti-CD28 antibody (clone CD28.2; Invitrogen) in 96-well, round-bottom plates. After 72 hours of stimulation, harvested cells were subjected to surface staining with fixable viability stain FVS V450, APC-H7 anti-CD3, PercP anti-CD4, V500 anti-CD8 (all from BD Biosciences), and PE-Cy7 PD-1 (Biolegend). Intracellular staining for Alexa Fluor 488 Ki67, PE IFN-γ, and Alexa Fluor 700 granzyme B was carried out after fixation and permeabilization of cells, and samples were acquired on an LSRII flow cytometer (BD Biosciences) (45). Data were analyzed using FlowJo 10.03 (Tree Star Inc.). Frequency and phenotype of Tregs, MDSCs, and $PD\text{-}1^+$

T cells were determined by polychromic flow cytometry as described before (8, 45).

Statistics. This study was a nonrandomized longitudinal study of biomarker changes from baseline to days 28–35 and day 160 following sorafenib therapy in 30 subjects. The primary endpoints were PFS and OS as a function of baseline biomarker levels and changes from baseline to days 28–35. Biomarker values were dichotomized for baseline values as above or below the median and above or below the median log change scores. Comparisons between the 2 strata were carried out using a log-rank test, tested at $\alpha = 0.05$ (2 sided). Differences in mean biomarker changes over time were examined using a paired *t* test at $\alpha = 0.05$ (2 sided). *P* values of less than 0.05 were considered significant. A time-varying Cox regression model was used to examine biomarker changes across the longitudinal time points in terms of relative risk of death over time.

Study approval. The study protocol (I 238913) was approved by the Roswell Park Institutional Review Board. Every patient signed an informed consent document in a manner consistent with the World Medical Association's Declaration of Helsinki and RPCCC standards to be included in this prospective, open-label biomarker study.

Author contributions

SGK and YT conceived and designed the study, developed the methodology, and acquired data. SGK, JB, AH, and YT analyzed and interpreted data. SGK, JB, RI, and YT wrote, reviewed, and revised the manuscript.

Acknowledgments

We would like to thank Catherine Grande, clinical research coordinator, and Deeponpaul Singh, clinical research associate, for the coordination of protocol amendment and quarterly status reports submissions. We also thank Adrienne Groman for her work on this project in data assemblage and quality control. This study was approved and funded by the National Comprehensive Cancer Network Oncology Research Program from general research support provided by Bayer U.S. LLC (NCCNSORA0002 to YT and RI) and National Cancer Institute grant P30CA016056 involving the use of RPCCC's Shared Resources. The studies on neuritin expression were supported by pilot funds from Roswell Park Alliance Foundation to JB and YT.

Address correspondence to: Yasmin Thanavala, Roswell Park Comprehensive Cancer Center, Elm and Carlton Streets, Buffalo, New York 14263, USA. Phone: 716.845.8536; Email: yasmin.thanavala@roswellpark.org.

1. El-Serag HB, Kanwal F. Epidemiology of hepatocellular carcinoma in the United States: where are we? Where do we go? *Hepatology*. 2014;60(5):1767–1775.
2. Llovet JM, et al. Hepatocellular carcinoma. *Nat Rev Dis Primers*. 2016;2:16018.
3. Sanyal AJ, Yoon SK, Lencioni R. The etiology of hepatocellular carcinoma and consequences for treatment. *Oncologist*. 2010;15(suppl 4):14–22.
4. Forner A, Reig M, Bruix J. Hepatocellular carcinoma. *Lancet*. 2018;391(10127):1301–1314.
5. Kudo M. Immune checkpoint inhibition in hepatocellular carcinoma: basics and ongoing clinical trials. *Oncology*. 2017;92(suppl 1):50–62.
6. Prieto J, Melero I, Sangro B. Immunological landscape and immunotherapy of hepatocellular carcinoma. *Nat Rev Gastroenterol Hepatol*. 2015;12(12):681–700.
7. Fu J, et al. Increased regulatory T cells correlate with CD8 T-cell impairment and poor survival in hepatocellular carcinoma patients. *Gastroenterology*. 2007;132(7):2328–2339.
8. Kalathil S, Lugade AA, Miller A, Iyer R, Thanavala Y. Higher frequencies of GARP(+)CTLA-4(+)Foxp3(+) T regulatory cells and myeloid-derived suppressor cells in hepatocellular carcinoma patients are associated with impaired T-cell functionality. *Cancer Res*. 2013;73(8):2435–2444.
9. Hoechst B, et al. A new population of myeloid-derived suppressor cells in hepatocellular carcinoma patients induces CD4(+)CD25(+)Foxp3(+) T cells. *Gastroenterology*. 2008;135(1):234–243.
10. Kalathil SG, Thanavala Y. High immunosuppressive burden in cancer patients: a major hurdle for cancer immunotherapy. *Cancer Immunol Immunother*. 2016;65(7):813–819.
11. Kalathil SG, Lugade AA, Miller A, Iyer R, Thanavala Y. PD-1$^+$ and Foxp3$^+$ T cell reduction correlates with survival of HCC patients after sorafenib therapy. *JCI Insight*. 2016;1(11):e86182.
12. Voron T, et al. VEGF-A modulates expression of inhibitory checkpoints on CD8$^+$ T cells in tumors. *J Exp Med*.

2015;212(2):139–148.
13. Klein O, et al. Flt3 ligand expands CD4+ FoxP3+ regulatory T cells in human subjects. *Eur J Immunol*. 2013;43(2):533–539.
14. Fouladi F, et al. Sorafenib induces paradoxical phosphorylation of the extracellular signal-regulated kinase pathway in acute myeloid leukemia cells lacking FLT3-ITD mutation. *Leuk Lymphoma*. 2015;56(9):2690–2698.
15. Soiffer RJ, Davids MS, Chen YB. Tyrosine kinase inhibitors and immune checkpoint blockade in allogeneic hematopoietic cell transplantation. *Blood*. 2018;131(10):1073–1080.
16. Cabrera R, et al. The anti-viral effect of sorafenib in hepatitis C-related hepatocellular carcinoma. *Aliment Pharmacol Ther*. 2013;37(1):91–97.
17. Chen ML, et al. Sorafenib relieves cell-intrinsic and cell-extrinsic inhibitions of effector T cells in tumor microenvironment to augment antitumor immunity. *Int J Cancer*. 2014;134(2):319–331.
18. Cao M, et al. Kinase inhibitor Sorafenib modulates immunosuppressive cell populations in a murine liver cancer model. *Lab Invest*. 2011;91(4):598–608.
19. Wang Q, et al. Sorafenib reduces hepatic infiltrated regulatory T cells in hepatocellular carcinoma patients by suppressing TGF-β signal. *J Surg Oncol*. 2013;107(4):422–427.
20. Cabrera R, et al. Immune modulation of effector CD4+ and regulatory T cell function by sorafenib in patients with hepatocellular carcinoma. *Cancer Immunol Immunother*. 2013;62(4):737–746.
21. Kalathil SG, Lugade AA, Iyer R, Miller A, Thanavala Y. Endothelial progenitor cell number and ERK phosphorylation serve as predictive and prognostic biomarkers in advanced hepatocellular carcinoma patients treated with sorafenib. *Oncoimmunology*. 2016;5(10):e1226718.
22. Abou-Alfa GK, et al. Phase II study of sorafenib in patients with advanced hepatocellular carcinoma. *J Clin Oncol*. 2006;24(26):4293–4300.
23. Liang Y, et al. Phosphorylated ERK is a potential prognostic biomarker for Sorafenib response in hepatocellular carcinoma. *Cancer Med*. 2017;6(12):2787–2795.
24. Kudo M. Immuno-oncology in hepatocellular carcinoma: 2017 update. *Oncology*. 2017;93(suppl 1):147–159.
25. El-Khoueiry AB, et al. Nivolumab in patients with advanced hepatocellular carcinoma (CheckMate 040): an open-label, non-comparative, phase 1/2 dose escalation and expansion trial. *Lancet*. 2017;389(10088):2492–2502.
26. Stein S, et al. Safety clinical activity of 1L atezolizumab + bevacizumab in a phase Ib study in hepatocellular carcinoma (HCC). *J Clin Oncol*. 2018; 36(suppl 15):4074–4074.
27. Chaudhary B, Elkord E. Regulatory T cells in the tumor microenvironment and cancer progression: role and therapeutic targeting. *Vaccines (Basel)*. 2016;4(3):E28.
28. Liu D, et al. Sunitinib represses regulatory T cells to overcome immunotolerance in a murine model of hepatocellular cancer. *Oncoimmunology*. 2017;7(1):e1372079.
29. Alberts R, et al. Expression QTL mapping in regulatory and helper T cells from the BXD family of strains reveals novel cell-specific genes, gene-gene interactions and candidate genes for auto-immune disease. *BMC Genomics*. 2011;12:610.
30. Bettini ML, et al. Loss of epigenetic modification driven by the Foxp3 transcription factor leads to regulatory T cell insufficiency. *Immunity*. 2012;36(5):717–730.
31. Gavin MA, et al. Foxp3-dependent programme of regulatory T-cell differentiation. *Nature*. 2007;445(7129):771–775.
32. Hill JA, et al. Foxp3 transcription-factor-dependent and -independent regulation of the regulatory T cell transcriptional signature. *Immunity*. 2007;27(5):786–800.
33. Kwon HK, Chen HM, Mathis D, Benoist C. Different molecular complexes that mediate transcriptional induction and repression by FoxP3. *Nat Immunol*. 2017;18(11):1238–1248.
34. Grinberg-Bleyer Y, et al. NF-κB c-Rel is crucial for the regulatory T cell immune checkpoint in cancer. *Cell*. 2017;170(6):1096–1108.e13.
35. Barbi JJ, Vignali PDA, Yu H, Pan F, Pardoll D. The neurotrophic factor neuritin maintains and promotes the function of regulatory T cells in autoimmunity and cancer. *J Immunol*. 2016;196(suppl 1):58.12.
36. Lin YC, et al. Activated but not resting regulatory T cells accumulated in tumor microenvironment and correlated with tumor progression in patients with colorectal cancer. *Int J Cancer*. 2013;132(6):1341–1350.
37. Luo CT, Liao W, Dadi S, Toure A, Li MO. Graded Foxo1 activity in Treg cells differentiates tumour immunity from spontaneous autoimmunity. *Nature*. 2016;529(7587):532–536.
38. Williams JB, Horton BL, Zheng Y, Duan Y, Powell JD, Gajewski TF. The EGR2 targets LAG-3 and 4-1BB describe and regulate dysfunctional antigen-specific CD8+ T cells in the tumor microenvironment. *J Exp Med*. 2017;214(2):381–400.
39. Zheng Y, et al. Egr2-dependent gene expression profiling and ChIP-Seq reveal novel biologic targets in T cell anergy. *Mol Immunol*. 2013;55(3-4):283–291.
40. Sia D, et al. Identification of an immune-specific class of hepatocellular carcinoma, based on molecular features. *Gastroenterology*. 2017;153(3):812–826.
41. Mathew NR, et al. Sorafenib promotes graft-versus-leukemia activity in mice and humans through IL-15 production in FLT3-ITD-mutant leukemia cells. *Nat Med*. 2018;24(3):282–291.
42. Christiansson L, et al. The tyrosine kinase inhibitors imatinib and dasatinib reduce myeloid suppressor cells and release effector lymphocyte responses. *Mol Cancer Ther*. 2015;14(5):1181–1191.
43. Kreutzman A, Ilander M, Porkka K, Vakkila J, Mustjoki S. Dasatinib promotes Th1-type responses in granzyme B expressing T-cells. *Oncoimmunology*. 2014;3:e28925.
44. Balachandran VP, et al. Imatinib potentiates antitumor T cell responses in gastrointestinal stromal tumor through the inhibition of Ido. *Nat Med*. 2011;17(9):1094–1100.
45. Kalathil SG, et al. T-regulatory cells and programmed death 1+ T cells contribute to effector T-cell dysfunction in patients with chronic obstructive pulmonary disease. *Am J Respir Crit Care Med*. 2014;190(1):40–50.